RECEIVED BY OSTI NOV 27 1985
CONF-850942--

RECENT DEVELOPMENTS AT TRISTAN: NUCLEAR STRUCTURE STUDIES OF NEUTRON-RICH NUCLEI

BNL--37156
DE86 003380

R. L. Gill
Brookhaven National Laboratory, Upton, New York, 11973, USA

Abstract

The nuclear physics program at the fission product mass separator, TRISTAN, has greatly expanded, both in the types of experiments possible and in the range of nuclei available. Surface ionization, FEBIAD, high-temperature thermal, high-temperature plasma, and negative surface ionization ion sources are routinely available. Experimental facilities developed to further expand the capabilities of TRISTAN include a superconducting magnet for g factor and Q_β measurements, a windowless Si(Li) detector for conversion electron measurements, and a colinear fast-beam dye laser system for hyperfine interaction studies. This combination of ion sources, experimental apparatus, and the long running time available at a reactor makes TRISTAN a powerful tool for nuclear structure studies of neutron-rich nuclei. The effect of these developments on the nuclear physics program at TRISTAN will be discussed and recent results from some of these facilities will be presented.

The TRISTAN Facility

A schematic layout of the TRISTAN ISOL facility is shown in Fig. 1. A neutron beam of about 3×10^{10} $n_{th}/cm^2/sec$ is provided by the 60 MW High Flux Beam Reactor at Brookhaven National Laboratory. Targets which typically contain 5g ^{235}U inside an ion source are positioned in the neutron beam to provide intense beams of short-lived neutron-rich nuclei produced by fission. To provide for maximum versatility, a variety of ion sources are used, each of which is best suited to producing certain elements [SHM83, GIL85, PIO84].

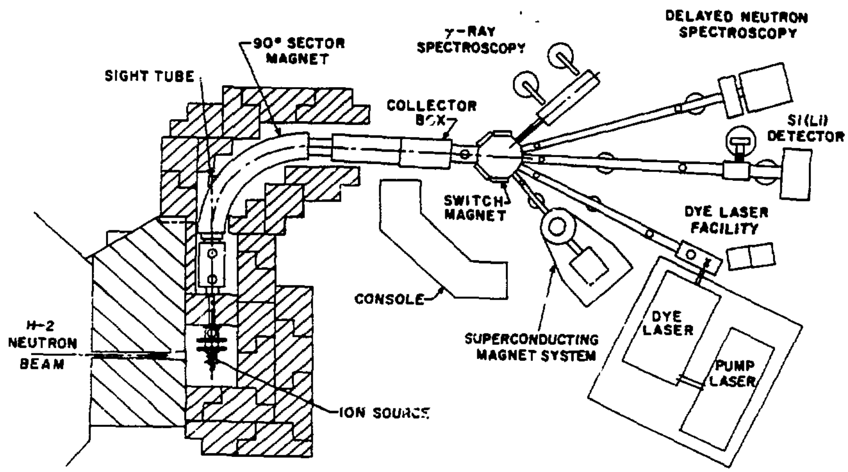

Fig. 1. Layout of the TRISTAN facility.

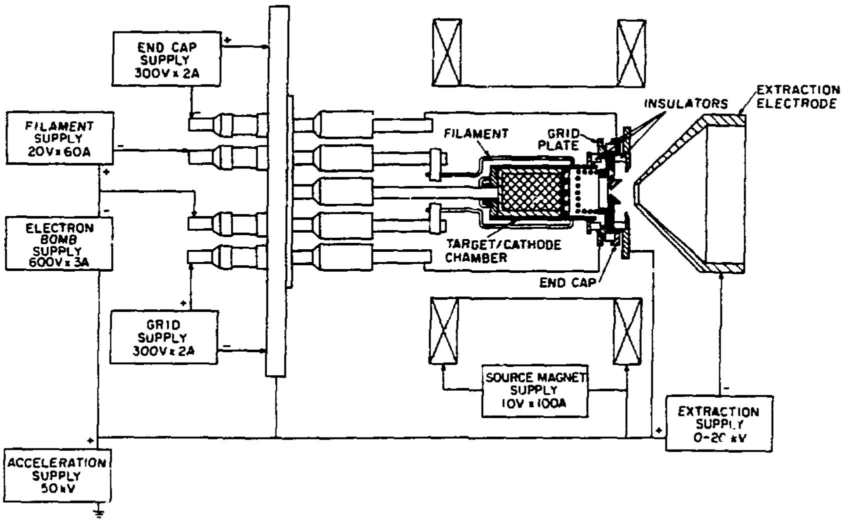

Fig. 2. Schematic diagram of the high temperature plasma ion source.

High Temperature Plasma Ion Source

The most recently developed ion source is the high temperature plasma ion source. The source is shown in Fig. 2. It is constructed in a fashion similar to the thermal and negative ion sources in that these three sources share a common design for the target, heating filamental heat shields. Thus, mass production and assembly of the sources has been simplified owing to standardization of the designs. Off-line studies have shown that this ion source exhibits ionization efficiencies of up to 60% for Kr and Xe in the low pressure limit. This source produces the same variety of elements as the FEBIAD source, but due to the larger target, higher temperature and high ionization efficiency, the intensities of the radioactive beams are significantly higher than with the FEBIAD source.

Experimental Facilities

In Fig. 1, the facilities available at each of the five beam ports at TRISTAN are labeled. The facilities are described in [GIL85] and references therein. The Si(Li) detector and superconducting magnet systems have become fully operational and widely used in the past year. These two facilities will now be described in some detail.

Si(Li) Detector. A windowless Si(Li) detector for conversion electron spectroscopy is housed in a cryostat with a compressable bellows connected to a vacuum chamber and moving tape collector. The detector can be moved to within 5 mm of the surface of an aluminized mylar tape on which radioactive ion beams are implanted. The tape system can be configured so that the ion beam deposition point is directly viewed by the detector or is located in an area shielded from the detector. In the latter configuration, the tape must be moved before the Si(Li) detector can view the source. One problem encountered when doing conversion electron spectroscopy with neutron-rich nuclei is the tendency of the β continuum to obscure the desired peaks. This interference can be suppressed by employing various gating techniques. A thin plastic scintillator (with very low γ-ray response) is used to suppress the β signal in the Si(Li) detector. The system is designed such that a standard Ge detector cryostat also views the same source as the Si(Li) detector. Thus, γ-ray electron and x-ray electron coincidences can also be employed to enhance the electron signal, as well as provide for element identification. In addition to these coincidence capabilities, electron and γ-ray singles can be simultaneously acquired, making it possible to measure internal conversion coefficients. The system has been used to identify weakly populated 0^+ states in $^{96,98}Zr$.

Superconducting Magnet. A split-pole, Nb-Ti superconducting magnet system, manufactured by Oxford Instruments, is available at TRISTAN for g-factor and Q_β measurements. The magnet has a field strength of 5.23 T at 108 A at 4°K with a homogeneity of <1 over 1 cm^2. A rectangular cross section room temperature tube penetrates the magnet bore to provide access for the tape from a moving tape collector. The magnet was designed to provide for maximum flexibility of detector positioning. An angle of 125° on each side of the base tube is free of significant γ-ray absorbing material. Detectors on opposite sides of the bore tube can be positioned as close as 90° to one another and as close as 9 cm to the source. An alignment jig was constructed to provide accurate angular positioning of each detector and support for shielding.

The magnet can also be used for $Q_β$ measurements. By placing a hyperpure Ge detector in a magnetic field, electrons from the source can be focussed onto the surface of the detector, thus providing a large effective solid angle for betas. At the same time, the detector can be far from the source, giving a low solid angle for γ rays. Such an arrangement is possible with the TRISTAN magnet. The lower pole piece can be removed and a LN_2 cooled heat shield is replaced by a cold finger containing the detector. Thus the magnet configuration can be changed without major disassembly of the system. Using this system, it is possible to obtain enhancements of electrons over γ rays by a factor of 15.

The tape collector for the superconducting magnet facility was designed and constructed at Brookhaven. It consists of a box with a large number of low friction rollers which guide the tape through the deposit port, into the magnet, through a series of loops, and to a stepping motor drive sprocket. The system contains about 15 m of tape. The tape is standard 16-mm movie film leader which has a layer of aluminum evaporated onto one side. Repairs to the tape are made with a standard film splicer. The drive sprocket was custom made since a much larger than standard diameter was desired to obtain maximum speed of the tape. The tape moves 362 mm to move a source from the deposit box to the center of the magnet. This can be accomplished in about 0.3 s with an error of less than 0.5 mm. A small surface barrier detector is provided to monitor the ion beam intensity.

The superconducting magnet system is equipped with several interlocks. One senses the external magnetic field and will give a signal if the field diminishes below a preset value, another senses a loss of vacuum in the tape collector and a third senses a broken tape condition. Each of the sensors will sound an alarm, stop the tape collector cycling, isolate the vacuum system, and stop data acquisition on the appropriate channels upon receiving a fault signal.

G-factor Measurements at TRISTAN

Using the superconducting magnet described above, g-factors of the 2^+_1 states in $^{146,148}Ce$ have been measured. In previous measurements [WOL83] at TRISTAN, using a conventional magnet, 2^+_1 states in Ba isotopes were measured and interpreted in terms of changes in the number of valence protons due to a subshell closure at Z=64. It was realized that the Ce isotopes would provide a more severe test of these ideas, since they would be the lowest Z isotopes for which an abrupt change in valence proton number could be observed in this region. However, due to the short lifetimes for the levels (0.25 ns for ^{146}Ce and 1.07 ns for ^{148}Ce) and the lower yields, a superconducting magnet system was crucial to the measurement.

The g-factors in $^{146,148}Ce$ were measured using the integral perturbed angular correlation technique where the intensity of the cascading γ rays (in these cases for a 0^+-2^+-0^+ cascade) are measured at an appropriate angle for field up and field down. The standard double ratio technique is used [WOL83] since this technique eliminates most systematic errors. The results obtained are: $g(2^+_1) = (0.24 \pm 0.05)$ for ^{146}Ce and $g(2^+_1) = (0.37 \pm 0.06)$ for ^{148}Ce. In IBA-2 formalism, the g-factor of the first 2^+ state in an even-even nucleus can be described by [SAM84] $g(2^+_1) = g_\pi N_\pi/N_t + g_\nu N_\nu/N_t$, where $N_t = N_\pi + N_\nu$. If the experimental values of $g(2^+_1)$ for isotopes of Ba-Dy are used to plot $g(2^+_1)\ N_t/N_\nu$ versus N_π/N_ν, a straight line is obtained with significant deviations being observed only for those isotopes expected to exhibit a truncated proton valence space due to the subshell closure at Z=64. Additionally, all of the deviations are in a direction that indicates a <u>smaller</u> proton valence space. If only those isotopes with N>90 are included in the fit $g_\pi = 0.63 \pm 0.04$ and $g_\nu = 0.05 \pm 0.05$ is obtained. If these empirically determined values of g_π and g_ν are accepted as being <u>constant</u> over a wide range of nuclei in this region, then the experimentally determined g-factors can be used as a measure of the effective number of valence protons (N_π in IBA-2 formalism). The results of this analysis are shown in Fig. 3 for Ba, Ce, Nd, and Sm isotopes. The dashed line shows the value of N_π expected for major shell closures from Z=50-82 (Z=82) and from Z=50-64 (Z=64) and the solid line indicates the region of transition between shells [GIL82]. The figure shows not only the distinct change in N_π, but also a tendency of the N_π change to shift to lower neutron number as Z increases. This

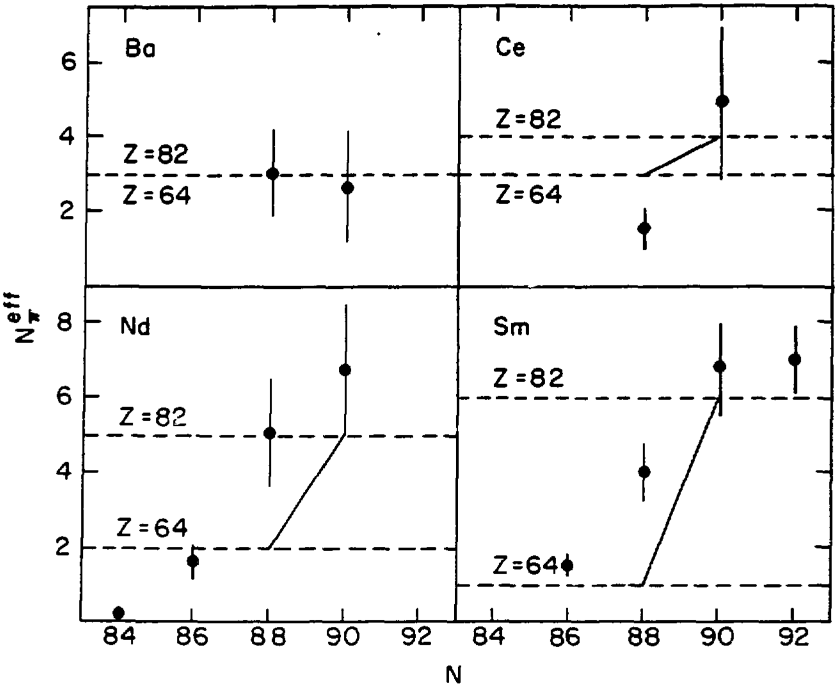

Fig. 3. N_π^{eff} deduced for isotones of Ba, Ce, Nd, and Sm. The Ba, Nd, and Sm data are from [WOL83] and references therein. The Ce data is from this work.

effect is primarily due to earlier occupation of the $\pi h_{11/2}$ orbital becoming possible as higher orbitals are filled with increasing Z. The neutron-proton interaction can then operate to the fullest extent (neutrons are occupying the $h_{9/2}$ orbital) resulting in a deformed nucleus having the lowest energy.

Acknowledgement

Research supported under contract DE-AC02-76CH00016 with the U.S. DOE.

References

[SHM83] M. Shmid et al., NIM 211 287 (1983).

[GIL85] R. L. Gill and A. Piotrowski, NIM 234 213 (1985).

[PIO84] A. Piotrowski et al., NIM 224 1 (1984).

[WOL83] A. Wolf et al., Phys. Lett. 123B 165 (1983).

[SAM84] M. Sambataro et al., Nucl. Phys. A423 333 (1984).

[GIL82] R. L. Gill et al., Phys. Lett. 118B 251 (1982).

DISCLAIMER